UNCLASSIFIED

SECURITY CLASSIFICATION OF THIS PAGE (When Data Entered)

(7)

AD-A134168

REPORT DOCUMENTATION PAGE		READ INSTRUCTIONS BEFORE COMPLETING FORM
1. REPORT NUMBER AFGL-TR-83-0272	2. GOVT ACCESSION NO. AD-A134168	3. RECIPIENT'S CATALOG NUMBER
4. TITLE (and Subtitle) Stratospheric Determination of Effective Photodissociation Cross Sections for Molecular Oxygen: 191-204 nm.		5. TYPE OF REPORT & PERIOD COVERED Final 1 Oct. 82-30 Sept. 83 6. PERFORMING ORG. REPORT NUMBER
7. AUTHOR(s) G.P. Anderson and L.A. Hall		8. CONTRACT OR GRANT NUMBER(s)
9. PERFORMING ORGANIZATION NAME AND ADDRESS Air Force Geophysics Laboratory (LIU) Hanscom AFB Massachusetts 01731		10. PROGRAM ELEMENT, PROJECT, TASK AREA & WORK UNIT NUMBERS 62101F 66870308
11. CONTROLLING OFFICE NAME AND ADDRESS Air Force Geophysics Laboratory (LIU) Hanscom AFB Massachusetts 01731		12. REPORT DATE 20 October 1983 13. NUMBER OF PAGES 20
14. MONITORING AGENCY NAME & ADDRESS(if different from Controlling Office)		15. SECURITY CLASS. (of this report) UNCLASSIFIED 15a. DECLASSIFICATION DOWNGRADING SCHEDULE

16. DISTRIBUTION STATEMENT (of this Report)

Approved for public release; distribution unlimited.

17. DISTRIBUTION STATEMENT (of the abstract entered in Block 20, if different from Report)

18. SUPPLEMENTARY NOTES

Presented at XVIII General Assembly of the International Union of Geodesy and Geophysics in Hamburg, F.R.G. - August 1983

19. KEY WORDS (Continue on reverse side if necessary and identify by block number)

Solar UV absorption
Stratosphere
Molecular Oxygen
Schumann-Runge region
Cross-sections

20. ABSTRACT (Continue on reverse side if necessary and identify by block number)

Balloon-borne spectrometer measurements of solar ultraviolet irradiance have been used to provide direct estimates of effective photodissociation cross-sections (σ_i^e, i = $\Delta\lambda$ interval) for molecular oxygen appropriate for altitudes between 30 and 40 km. The calculations from which σ_i^e can be determined are based on an internally consistent, two-part analysis of ascent spectra. The fine resolution O_2 absorption cross section derived from the fractional transmission between two altitudes is convolved with the calibrated insitu irradiances

DD FORM 1 JAN 73 1473 EDITION OF 1 NOV 65 IS OBSOLETE

UNCLASSIFIED

SECURITY CLASSIFICATION OF THIS PAGE (When Data Entered)

and then integrated over wavelength, yielding photodissociation rate coefficients (J-values) for the conditions of the flight: 22 April 1981 at 33°N latitude and approximately 50° solar zenith angle. The J-values are then decomposed into the σ_i^e and average attenuated irradiances for the selected wavelength intervals. Photochemical models which incorporate these altitude-dependent O_2 cross sections will reasonably approximate both the local optical attenuation and the photodissociation rate coefficients, since the σ_i^e have been calculated by a simultaneous solution of both the attenuation and the photodissociation equations.

The spectral data used in this study had sufficient resolution to record details in the rotational structure of the Schumann-Runge bands. The effective cross sections, however, are independent of the instrument resolution and agree well with other published theoretical and experimental values.

AFGL-TR-83-0272

Stratospheric Determination of Effective Photodissociation Cross Sections for Molecular Oxygen: 191-204 nm

G.P. Anderson and L.A. Hall

Abstract

Balloon-borne spectrometer measurements of solar ultraviolet irradiance have been used to provide direct estimates of effective photodissociation cross sections (σ_i^e, i = $\Delta\lambda$ interval) for molecular oxygen appropriate for altitudes between 30 and 40 km. The calculations from which σ_i^e can be determined are based on an internally consistent, two-part analysis of ascent spectra. The fine resolution O_2 absorption cross section derived from the fractional transmission between two altitudes is convolved with the calibrated insitu irradiances and then integrated over wavelength, yielding photodissociation rate coefficients (J-values) for the conditions of the flight: 22 April 1981 at 33°N latitude and ~ 50° solar zenith angle. The J-values are then decomposed into the σ_i^e and average attenuated irradiances for the selected wavelength intervals. Photochemical models which incorporate these altitude-dependent O_2 cross sections will reasonably approximate both the local optical attenuation and the photodissociation rate coefficients, since the σ_i^e have been calculated by a simultaneous solution of both the attenuation and the photodissociation equations.

The spectral data used in this study had sufficient resolution to record details in the rotational structure of the Schumann-Runge bands. The effective cross sections, however, are independent of the instrument resolution and agree well with other published theoretical and experimental values.

I. Introduction:

The photochemical behavior of the stratosphere relies strongly on the depth of penetration of solar ultraviolet irradiance, especially over the wavelength intervals in which the dissociation of molecular oxygen occurs. The band structure and magnitude of the O_2 absorption cross section between 190 and 240 nm, coupled with attenuation by O_3, governs the transmission and deposition of energy to altitudes as low as 20 km.[1] Balloon-borne experiments, including photometer measurements by Brewer and Wilson[2] and more recent data from spectrometers[3,4,5], (Anderson & Hall, 1983, ref. 5, will subsequently be referred to as [A-H]), suggest that the transmission in this wavelength range, particularly near 200 nm, is greater than expected, indicating that the recommended[6] O_2 Herzberg continuum cross sections may be too large. Photochemical models which incorporate the smaller O_2 cross sections derived from stratospheric balloon data predict significantly different vertical profiles for ozone and several catalytic species.[1,7]

The accuracy of any balloon derivation of an O_2 cross section is predicated upon the reliability of previously measured O_3 cross sections[8] plus the correct in-flight detection of pressure and differential O_3 column amounts. Even with the sometimes large error estimates (10-30%) associated with the stratospheric data and analyses, the greater atmospheric transparency at 200 nm has been persistently observed.

These cross sections for absorption by molecular oxygen also enter directly into the calculation of photodissociation rate coefficients (J-values) which describe the efficiency of odd oxygen production at any altitude. In general,

$$J(z) = \int_{\lambda_1}^{\lambda_2} \sigma(\lambda)\, I(\lambda,z)\, d\lambda \qquad (1a)$$

where: $\sigma(\lambda)$ = photodissociation cross section of species being considered(O_2)

$$I(\lambda,z) = I_o(\lambda) \exp\left(-\sum \tau(\lambda,z)\right) = \qquad (1b)$$

attenuated solar irradiance available at altitude z

$I_o(\lambda)$ = unattenuated solar irradiance

$\sum \tau(\lambda,z)$ = total optical depth of intervening atmosphere, (1c) including nonvertical path length factor

λ_1, λ_2 = wavelength limits for the dissociation process or interval being considered,

Because of the complexity of the O_2 Schumann-Runge band system, whose cross section varies by orders of magnitude within .1 nm, the wavelength resolution required for this numerical integration is smaller than .01 nm. Excessive computer resources are required to incorporate such repetitive calculations, including the temperature dependencies and slant path variables, into stratospheric photochemical models. This realization has led to the development of various parameterizing schemes which approximate the integral with broad resolution solar irradiance measurements [$\bar{I}_o(\Delta\lambda)$] convolved with altitude-dependent effective absorption cross sections, $\sigma_{eff}(Z,\Delta\lambda)$,[9,10] (Allen & Frederick, 1982, ref. 10, will subsequently be referred to as [A-F].)

II. Objectives:

To the extent that balloon-borne spectrometers give both a direct measure of the attenuated local irradiance (equation 1b) and an in-situ derivation of the observed O_2 cross section at the instrument resolution, they can verify the predicted variations of the theoretically-based effective cross sections. In addition, within the error estimates of both the instrument calibration and the atmospherically derived cross sections, the balloon data can also provide an estimate of (1) photodissociation rate coefficients (equation 1a) for the particular flight conditions, (2) the unattenuated solar irradiance, ($I_o(\lambda)$), and (3) the more general J-values corrected to overhead sun conditions, for comparison with the theoretical estimates necessary in modelling efforts.

III. Experiment:

The present analysis is based primarily on the ascent data from the April 1981 flight of a single-dispersion, half-meter Ebert-Fastie spectrometer at Holloman Air Force Base, N.M. The instrument and flight characteristics for the experiment have been described in previous publications.[5,11] The two detectors, each with its own exit slit, optical path, and resolution, make simultaneous measurements over the wavelength range 191-310 nm. The wide and narrow slit resolutions are 0.1 and .012 nm respectively.

An O_2 absorption cross section has been extracted from the differential transmission between 33 and 39 km.[5] Because of dual contamination from the instrument (stray light) and the atmosphere (ozone), the absolute error estimates for that derived cross section were large ($\pm$30%). However, the relative errors were small, resulting in a cross section which exhibited feature-for-feature replication of much of the theoretically expected, pressure-broadened, Schumann-Runge band structure.

This relative accuracy provides a realistic opportunity to explore the implications of using "effective" cross sections as an approximation in atmospheric models.

On April 20, 1983, the same spectrometer was flown with a broad band filter modification which virtually eliminated instrumental scattered light for the narrow resolution detector. The preliminary data from that flight will be used to augment this study and tighten the error estimates.

IV. Theory:

As Allen and Frederick[10] point out, the detailed O_2 cross section, satisfies two simultaneous relationships. The first governs the attenuation of energy within a layer (Z_1-Z_2) such that at any wavelength:

$$I(Z_2) = I(Z_1) \cdot \exp(-\sigma(O_2) \cdot \Delta N(O_2)) \cdot \exp(-\Delta\tau(\text{other})) \qquad (2)$$

where: $I(Z)$ = measured irradiance at altitude Z

$\Delta N(O_2)$ = incremental increase in column density of O_2 between Z_1 and Z_2, including slant path factor

$\Delta\tau(\text{other})$ = incremental increase in optical depth due to non-O_2 processes, (O_3 and Rayleigh scattering), also including slant path factor.

The second relationship is the integral equation which defines the photodissociation rate coefficient for O_2 at altitude Z:

$$J(O_2, Z) = \int_{\lambda} \sigma(O_2)\, I(Z)\, d\lambda \qquad (3)$$

Using "standard atmosphere" approximations for ozone, pressure, and temperature profiles, plus the compilation of $\sigma(O_2)$ by Frederick & Hudson[13] at better than .004 nm resolution, [A-F] evaluate the exact $J_i(Z)$ over broad wavelength intervals and parameterize a set of effective cross sections, $\sigma_i^e(Z)$ which fit the altitude behavior of the exact solutions

and satisfy the criteria of equations 2 and 3, rewritten as:

$$I_i(Z_2) = I_i(Z_1) \cdot \exp(-\sigma_i^e(Z') \cdot \Delta N(O_2)) \cdot \exp(-\Delta\tau_i(\text{other})) \quad (4a)$$

$$J_i(Z_2) = \sigma_i^e(Z_2) \cdot I_i(Z_2) \cdot \Delta\lambda_i \quad (4b)$$

where: I_i = average solar irradiance over the λ_i interval and

$$\sigma_i^e(Z') = \frac{1}{2} \left(\sigma_i^e(Z_1) + \sigma_i^e(Z_2)\right) \sim \sigma_i^e(Z_1)$$

The appearance of the same $\sigma_i^e(Z)$ in both the exponential term of equation 4a and the linear term of equation 4b is based on the assumption that the O_2 optical depth over the selected wavelength interval and within the altitude layer is small (<1). Of course, the strong band excursions in the detailed O_2 cross section cause complete extinction to occur unevenly over the spectral and altitude intervals. The accuracy and altitude dependence of the effective cross sections rests then mostly on the choice of relatively small ΔZ increments. [A-F] could formulate almost continuous altitude profiles so this was not a problem. However, even with finite altitude intervals, the restriction is minimized because once the solar irradiance has been extinguished by a strong band within a wavelength interval, that band can make no further contribution to the local J-values or subsequent attenuation.

This same system of non-linear equations (2 & 3), involving $\sigma(O_2)$, can be explicitly evaluated using only the atmospheric balloon data. At high resolution the derived cross section encompasses the detail necessary for accurate integration of equation 3 to yield $J(O_2, Z)$. The integration limits are chosen to coincide with the wavelength intervals of the [A-F] effective cross sections. Substituting equation 4a into equation 4b gives:

$$\sigma_i^e(Z_2) \cdot \exp(-\sigma_i^e(Z_2) \cdot \Delta N(O_2) = \left[J_i(Z_2)/(I_i(Z_1)\right] \cdot e^{-\Delta\tau(\text{other})} \cdot \Delta\lambda_i \quad (5)$$

All the terms on the right hand side of equation 5 are readily determined from the measurements. The atmospherically derived $\sigma_i^e(Z_1)$ that can satisfy the non-linearities of equation 5 are the values to be compared to the published [A-F] results. Again, the accuracy of these experimentally derived $\sigma_i^e(Z)$'s is dependent on the thickness of the altitude layer and the strength of the incurred attenuation. For $\lambda>196$ nm, the differential O_2 optical depth is generally less than 2 for the imposed ΔZ of ~3 km. At shorter wavelengths where the Schumann-Runge bands become very strong, the accuracy falls accordingly.

To the extent that the atmospherically derived detailed cross section is measurable (usually within the dynamic range of 6×10^{-23} and 4×10^{-24} cm^2; see [A-H] for discussion), the total optical depth of the atmosphere can be estimated. Equation 1b can then be used to determine an $I_o(\lambda)$, the unattenuated solar irradiance, for any spectral scan. The repeatability of the spectral detail observed in these "top of the atmosphere" extrapolations lends credibility to the analysis scheme. At those wavelengths where it is possible to obtain an extrapolated $I_o(\lambda)$, more fundamental photodissociation rate coefficients can be formulated that describe the Schumann-Runge and Herzberg continuum behavior appropriate in the stratosphere under arbitrary atmospheric conditions, not just those of the flight.

V. Preliminary Results:

The wavelength intervals over which the effective cross section analysis has been attempted are those of Allen & Frederick[10] (Table I).

TABLE I

Interval	Range cm^{-1}	Range nm
1	48600 - 49000	204.1 - 205.8
2	49000 - 49500	202.0 - 204.1
3	49500 - 50000	200.0 - 202.0
4	50000 - 50500	198.0 - 200.0
5	50500 - 51000	196.1 - 198.0
6	51000 - 51500	194.2 - 196.1
7	51500 - 52000	192.3 - 194.2

The first step in the procedure requires the derivation of $\sigma(O_2)$ at fine resolution, as described in [A-H]. The detailed cross section is then convolved pointwise with the measured calibrated irradiances at each wavelength (500 points/nm at .012 nm resolution) and integrated over the selected intervals (eq. 3). This yields the photodissociation rate of O_2 over that interval for the atmospheric conditions of the particular spectral measurement. The inability to determine values of $\sigma(O_2)$ greater than 1×10^{-22} cm^2 (see [A-H) and previous discussion) is generally not important in that the coupled local irradiance measurement should be zero within a strong band. If, because of the instrumental scattering characteristics and noise, a true zero was not recorded by the spectrometer, a zero-fill value for that $I(\lambda,Z)$ was assigned [$I(\lambda,Z)\equiv 0$ if $\sigma(\lambda) > 1.E-22 cm^2$]. Such an approximation worked well for Schumann-Runge intervals 3,4, and 5. It was unnecessary for Herzberg continuum intervals 1 or 2 because at those wavelengths the atmosphere is optically

thin. However, for intervals 6 and 7, $J_i(Z)$ was significantly underestimated because of the coupled strong attenuation and relatively low signal-to-noise ratio.

For demonstration purposes the photodissociation rate coefficient for flight conditions over the wavelength interval 191-205 nm has been calculated and appears in figure 1a (heavy line). The error bars are ~ 30% at 3.2 mb.; the largest individual error source comes directly from the errors in the derived cross section. This particular curve results from the convolution of the detailed spectral measurements with the [A-H] cross section. However, if the instrument resolution had been coarser, the results would have been the same; that is, the data analysis, including the $\sigma(O_2)$ derivation, is internally consistent, relying only on the measured irradiances and the self-determined, instrumentally appropriate $\sigma(O_2)$.

The fine-line curve in figure 1a is an approximation of the photodissociation rate coefficients that would have been inferred from the spectral measurements <u>if</u> the sun had been overhead. This requires extrapolating back to the irradiance at the top of the atmosphere, $I_o(\lambda)$. The accuracy of $J(\Theta\equiv 0)$ depends on the degree to which that inference is appropriate, which is, of course, only at those wavelengths where $\Delta\tau(O_2)$ does not lead to complete attenuation. Figure 2 shows a portion of the solar irradiance in the optically thin Herzberg continuum region for two independent extrapolations, one from a scan at 39 km, the other from a scan at 37 km. The agreement is excellent; the features are repeatable Fraunhofer solar structure at ~ .02 nm resolution. The circles plotted for comparison, are sample .2 nm resolution values from Mount & Rottman[14] [M-R]. The straightline segments are 1 nm averages from [M-R] and this analysis. The $I_o(\lambda)$ values for this experiment average 10-15% higher

than the [M-R] values, but that difference is within the current large error estimates. In other wavelength intervals, where strong O_2 band structure occurs, the extrapolation is imprecise and may even be impossible.

As described in the theory section, the information contained in the vertical behavior of the irradiance depletion relative to the float measurements over broad wavelength intervals can be used to derive effective cross sections. Figure 1b (heavy line) shows $\sigma^e(Z)$ appropriate to flight conditions for the complete 191-205 nm interval. These altitude dependent values were calculated from equation 5 and satisfy equations 4a & b for that wavelength interval. The fine-line curve again is appropriate for overhead-sun conditions and at 3.2 mb (39 km) is normalized to the slant path value because of the lack of any additional information at higher altitudes. The differences between the Θ=0 extrapolation and the $\Theta > 45°$ measurements are real only at and below 33 km.

The arbitrary wavelength interval 191-205 nm demonstrates the basic vertical behavior of both the effective cross sections and related photodissociation rate coefficients. The $\sigma^e(Z)$ and $J(Z)$ will be the same within the instrumental error estimates, independent of instrument resolution. However, photochemical models need to accommodate smaller wavelength intervals because of possible solar variability, minor constituent absorption properties, etc. that may vary as a function of wavelength. Figure 3 (heavy lines) shows the results for wavelength intervals 2 through 6 (from Table 1) as derived from the atmospheric data. For comparison, the approximate [A-F] results (for overhead sun conditions) that encompass the altitude range of the measurements are also included. The curves for

σ_i^e (i = 2) (~ 202-204 nm) exhibit a similar lack of response to altitude changes in both the experimental and theoretical analysis, but the magnitudes differ by 40%. This behavior is attributable to the difference between the laboratory determinations of the Herzberg continuum used by [A-F], (see their discussion), and the atmospherically determined values. The new laboratory estimates of Yoshino et al.[15] are much closer to the low [A-H] values (~$8.5 \times 10^{-24} cm^2$ at 200 nm and ~$7.0 \times 10^{-24} cm^2$ at 203 nm, respectively).

In general, the vertical behavior for each interval approximates the theoretical predictions. Interval 3 includes most of the Schumann-Runge 1-0 band which is not considered to be predissociative in the [F-H] O_2 cross section compilation and is not incorporated in the [A-F] computations. If the measured band structure were removed and only the underlying continuum included in this analysis, the discrepancy would be slightly (< 10%) larger. Again, the fine-line curves denote the effective cross section for overhead sun, $\sigma_i^e(\theta \equiv 0)$, and are most accurate at 33 km and underestimated at 39 km [especially for the strong band intervals 5 (the 2-0 band) and 6 (the 3-0 band)]. The 4-0 and part of the 5-0 bands (intervals 7 & 8 respectively) are so optically thick that the results are not included in the figure, although they give reasonable results at 37 and 33 km (within 30% of the [A-F] values).

Because of the internal consistency of the data set, the general applicability of these derived effective cross sections can be tested directly against the measurements of the solar irradiance as it is attenuated within the atmosphere. Intervals 2 and 3 are sufficiently optically thin that $\sigma_i^e(i=2,3)$ can replace the exact cross sections in either equation 2 (as an exponential term) or equation 3 (as a linear term) with no dis-

cernible errors. Because intervals 4 and 5 center on portions of the relatively strong 2-0 Schumann-Runge band, the thickness of the altitude layers imposed by the experiment force those attenuation terms to become unevenly opaque. A comparison between the measured average irradiance at 33 km and the value predicted from equation 2, with σ_i^e (i=4,5) in the attenuation term and I_i(Z=39 km) as the unattenuated average irradiance, leads to an error of 4% for interval 4 and 8% for interval 5. At 37 km, the errors are 2 & 4% respectively. In each case the effective cross section accounted for too little attenuation. These differences, though small, would be significant in a modelling effort. The potential errors emanating from using σ_i^e(i=4,5) in equation 3 are small, leading to less than 4% differences in predicted vs. measured photodissociation rate coefficients, independent of altitude.

VI. Conclusions:

Effective cross sections appropriate for O_2 photodissociation rate calculations have been derived solely from in-situ measurements of stratospheric irradiance. The results agree well with the predicted vertical and zenith angle behavior suggested by Allen and Frederick[10]; the absolute magnitude differences, where they exceed the 30% experimental errors, can be attributed to differences in the adopted Herzberg continuum cross sections (relatively large laboratory values [A-F] vs. the relatively small values derived from the balloon data). In addition to the σ_i^e(Z)'s, this analysis also provides extrapolated estimates of $I_o(\lambda)$ whenever the optical depth at 39 km is < 1.0. Such extrapolations are, on average, 10-20% higher than the Mount and Rottman (1983) values, but still within the error estimates. The resultant photodissociation rates also agree with theoretical work[12] to within the error estimates, with a persistent tendency to be slightly higher.

This study was based primarily on data from the 1981 balloon flight which exhibited considerable optical contamination near 200 nm. The instrument has been reflown (4/20/83) with design modifications which significantly improved the signal-to-noise ratio. Figure 4 shows three spectral segments; 4a is a 1981 scan initiated at 33 km, 4b is a 1983 scan at the same approximate altitude, and 4c is a 1983 scan measured at float altitude (39 km). In the wavelength range 192.3 to 192.8 nm the atmosphere is optically thick because of the strong 4-0 bandhead and all three scans should measure zero (0) solar irradiance. In the 1981 analysis, the observed stray light background was estimated over that interval (and others) and removed (see [A-H]); this process is primarily responsible for introducing the large error estimates in the derived quantities. The full analysis described here, when applied to the 1983 data set, should yield more accurate results. A preliminary study has already shown that the low Herzberg continuum estimates will be reproduced.

In addition, solar variability in the critical ultraviolet window region has yet to be established. The 1983 flight, coupled with a reanalysis of the '77, '78, '80 and '81 flights, may lead to a definitive understanding of the natural oscillations of odd oxygen in general and some catalytic species in particular. This may shed additional light on the recuperative properties of the stratosphere.

Finally, recent theoretical work by Blake et al.[16] on the isotopic O_2 absorption properties, $(\sigma(O_{16}O_{18}))$, <u>may</u> be experimentally verified by a careful analysis of the '83 flight data. If this can be done, the importance of heavy O_2 and O_3 to the stratospheric chemical balance may be ascertained.

References

1. Brasseur, G., A. De Rudder and P.C. Simon, Implication for stratospheric composition of a reduced absorption cross section in the Herzberg continuum of molecular oxygen, Geophys. Res. Lett., 10, 20-23, 1983.

2. Brewer, A.W. and A.W. Wilson, Measurements of solar ultraviolet radiation in the stratosphere, Quart. J. Roy. Meteorol. Soc., 91, 452-461, 1965.

3. Frederick, J.E. and J.E. Mentall, Solar Irradiance in the Stratosphere: Implications for the Herzberg continuum absorption of O_2, Geophys. Res. Lett., 9, 461-464, 1982.

4. Herman, J.R. and J.E. Mentall, O_2 absorption cross sections (187-225 nm) from stratospheric solar flux measurements, J. Geophys. Res., 87, 8967-8975, 1982.

5. Anderson, G.P. and L.A. Hall, Attenuation of solar irradiance in the stratosphere: spectrometer measurements between 191 and 207 nm, J. Geophys. Res., in press, 1983.

6. World Meteorological Organization, The Stratosphere 1981: Theory and measurements, Rep. II, WMO Global Ozone Res. Monit. Proj., NASA/GSFC, Greenbelt, MD, 1982.

7. Froidevaux, L. and Y.L. Yung, Radiation and chemistry in the stratosphere: sensitivity to O_2 absorption cross sections in the Herzberg continuum, Geophys. Res. Lett., 9, 854-857, 1982.

8. Inn, E.C.Y. and Y. Tanaka, Absorption coefficient of ozone in the ultraviolet and visible regions, J. Opt. Soc. Am., 43, 870-873, 1953.

9. Park, J.H., The equivalent mean absorption cross sections for the O_2 SchumannRunge bands: Application to the H_2O and NO Photodissociation Rates, J. Atmos. Sci., 31, 1893-1997, 1974.

10. Allen, M. and J.E. Frederick, Effective photodissociation cross sections for molecular oxygen and nitric oxide in the Schumann-Runge bands, J. Atmos. Sci., 39, 2066-2075, 1982.

11. Hall, L.A., Solar ultraviolet irradiance at 40 kilometers in the stratosphere, J. Geophys. Res., 86, 555-560, 1981.

12. Frederick, J.E. and R.D. Hudson, Predissociation line widths and oscillator strengths for the 2-0 to 13-0 Schumann-Runge bands of O_2, J. Molec. Spectrocs., 74, 247-256, 1979.

13. Frederick, J.E. and R.D. Hudson, Dissociation of molecular oxygen in the SchumannRunge bands, J. Atmos. Sci., 37, 1099-1106, 1980.

14. Mount, G.H. and G.J. Rottman, The solar absolute spectral irradiance 11503173A: 17 May 1982, in press, J. Geophys. Res., 1983.

15. Yoshino, K., D.E. Freeman, J.R. Esmond and W.H. Parkinson, High resolution absorption cross section measurements and band oscillator strengths of the (1,0) (12,0) Schumann-Runge bands of O_2, Planet. Space Sci., 31, 33935, 1983.

16. Blake, A.J., D.G. McCoy, S.T. Gibson, Modelling atmospheric absorption in the Schumann-Runge region, Abstract, IAGA/IAMAP Joint Symposium on Middle Atmospheric Sciences, Hamburg, Germany, pg 187, 193.

Figure Captions

Figure 1a: Experimentally derived photodissociation rate coefficients for the full wavelength interval 191-205 nm.

Figure 1b: Experimentally derived effective cross sections for the same wavelength interval, appropriate for calculating both attenuation and photodissociation within the stratosphere.

Figure 2: Two independent measures of extrapolated solar irradiance (I_o) for the wavelength interval 2020-2040A. The repeatability of both the Fraunhofer structure and the absolute magnitude is excellent. For comparison the results of Mount & Rottman (1983) are also presented.

Figure 3: Experimentally derived effective cross sections for the wavelength intervals selected by Allen and Frederick (1982). See Table 1 for wavelength identifications. Because intervals 2 and 3 are located in the region of the Herzberg continuum, the lack of agreement with the theoretical work is expected (see text). The results for the other intervals all fall within the error estimates.

Figure 4: Comparison of solar irradiance spectral data from the 1981 and 1983 flights. The top (1981) and middle (1983) spectra were both measured near 33 km and have undergone similar atmospheric attenuation. However, the addition of a broad band filter to the spectrometer in the 1983 flight removed a significant noise source (as described in the text).

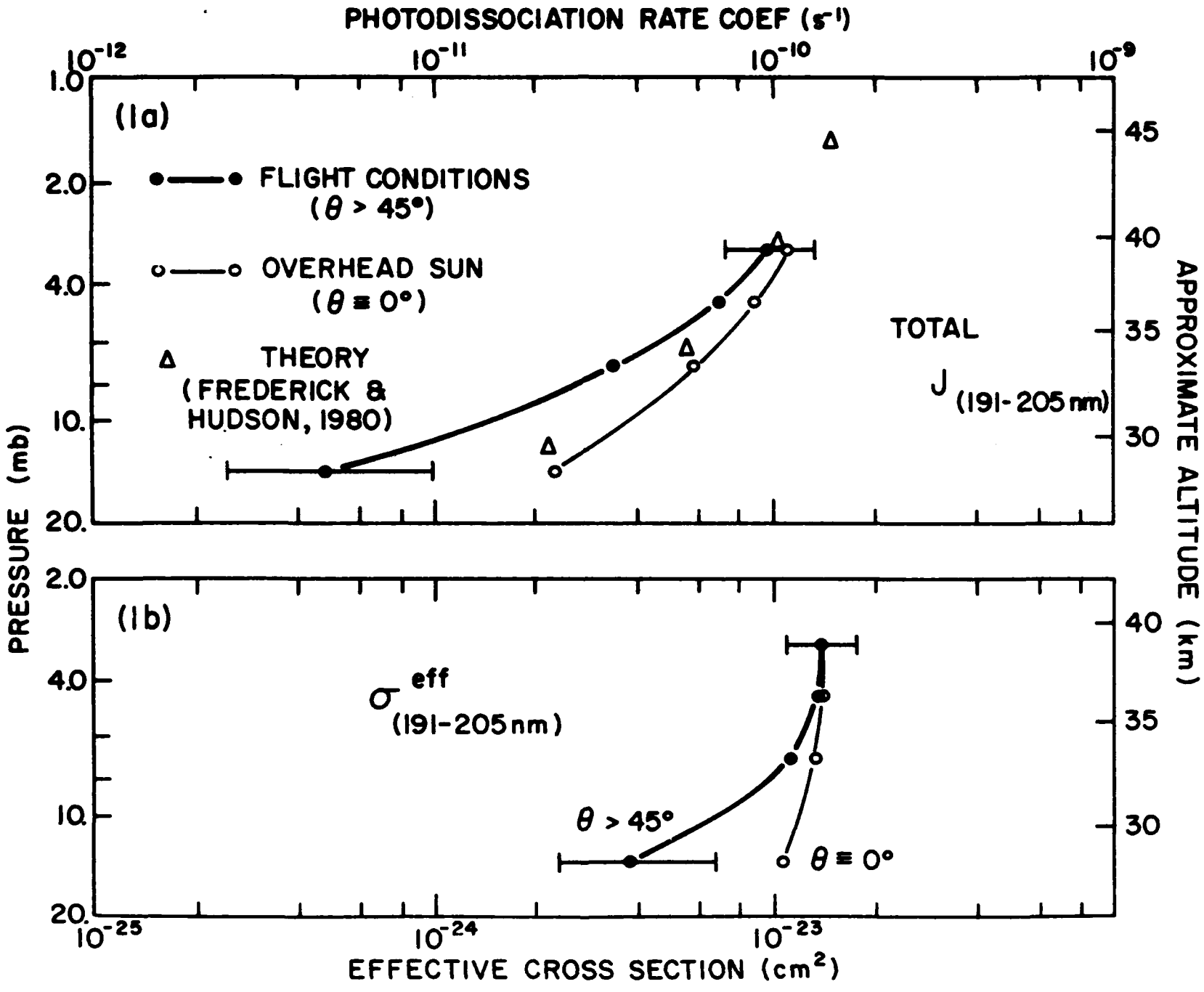
PHOTODISSOCIATION RATE COEF (s⁻¹)
10⁻¹²
10⁻¹¹
10⁻¹⁰
10⁻⁹
(1a)
FLIGHT CONDITIONS
(θ > 45°)
OVERHEAD SUN
(θ ≡ 0°)
THEORY
(FREDERICK & HUDSON, 1980)
TOTAL
J (191-205 nm)
PRESSURE (mb)
1.0
2.0
4.0
10.
20.
45
40
35
30
APPROXIMATE ALTITUDE (km)
(1b)
σ eff (191-205 nm)
θ > 45°
θ ≡ 0°
10⁻²⁵
10⁻²⁴
10⁻²³
EFFECTIVE CROSS SECTION (cm²)

Figure 1

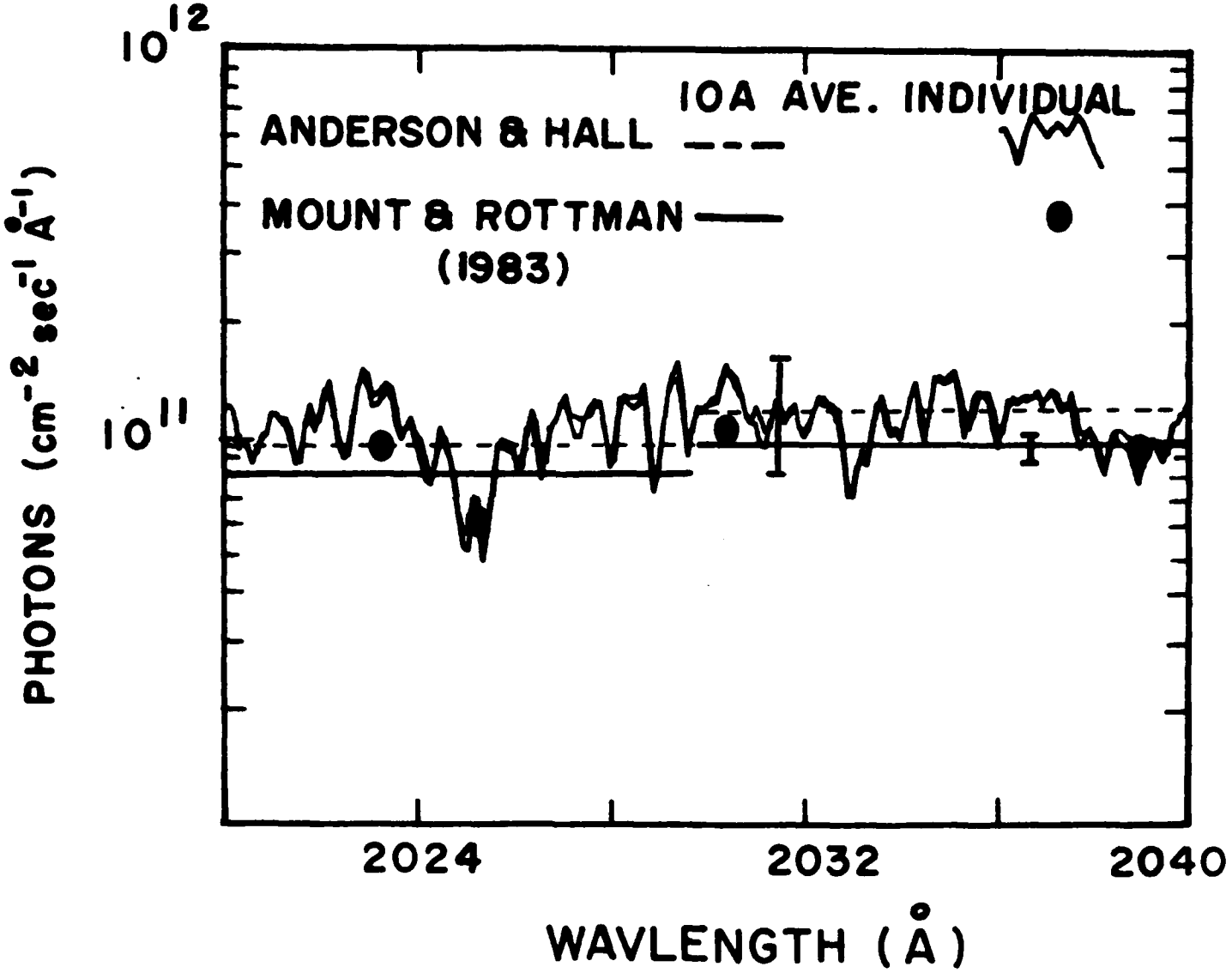
EXTRAPOLATED SOLAR IRRADIANCE
10^12
10^11
PHOTONS (cm^-2 sec^-1 Å^-1)
10A AVE. INDIVIDUAL
ANDERSON & HALL
MOUNT & ROTTMAN
(1983)
2024
2032
2040
WAVLENGTH (Å)

Figure 2

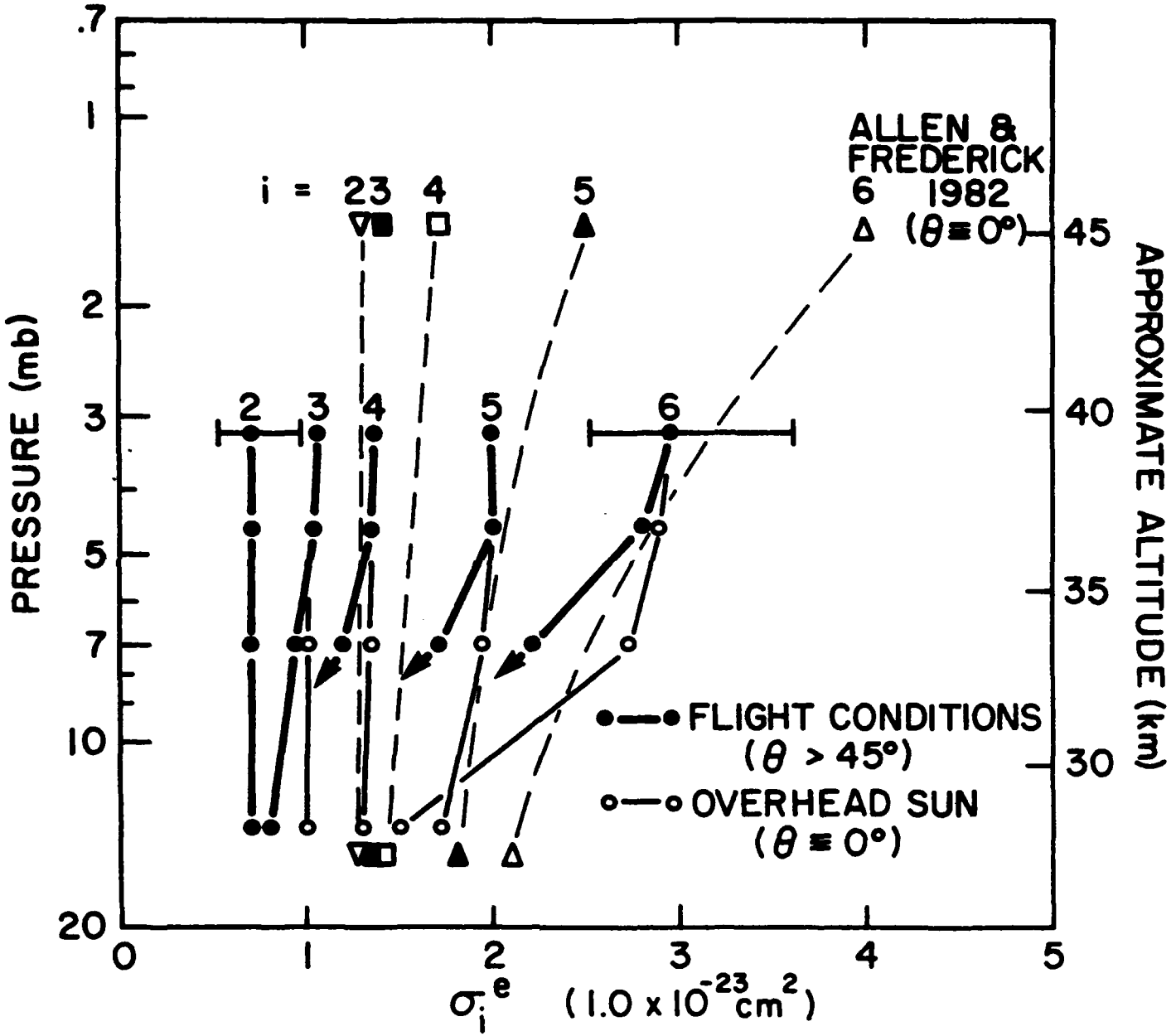
PRESSURE (mb)
.7
1
2
3
5
7
10
20
APPROXIMATE ALTITUDE (km)
45
40
35
30
0
1
2
3
4
5
σ_i^e (1.0 x 10^{-23} cm^2)
i = 23 4 5
2 3 4 5 6
ALLEN & FREDERICK 6 1982
Δ (θ ≡ 0°)
FLIGHT CONDITIONS (θ > 45°)
OVERHEAD SUN (θ ≡ 0°)

Figure 3

STRATOSPHERIC SOLAR IRRADIANCE (AFGL, HOLLOMAN AFB, N.M.)

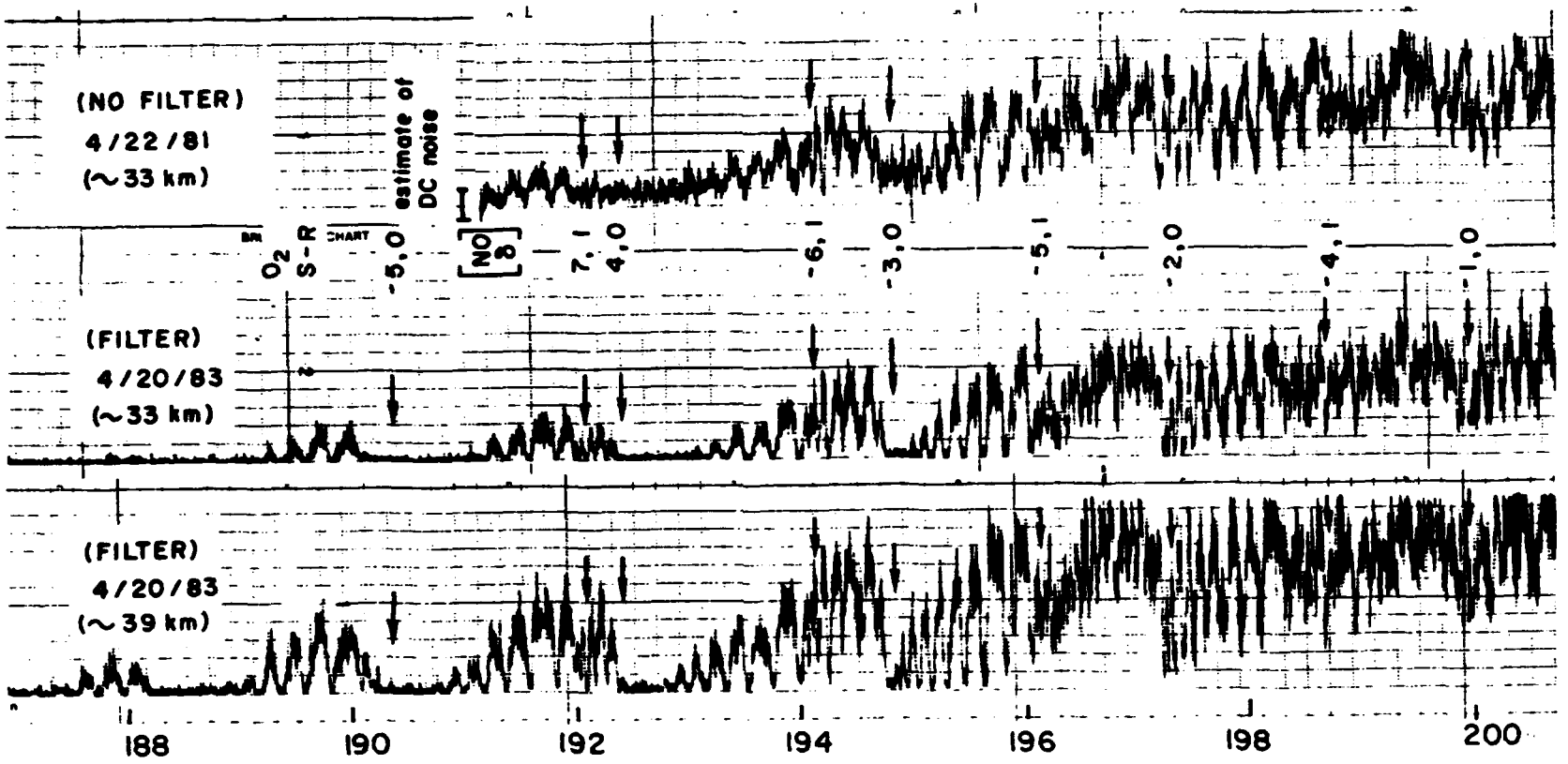

Figure 4